

# Microstructure-Based Modeling of Inner Oxygen Pressure in Solid Oxide Electrolysis Cells



*Fei Xue*

*Research Scientist/NETL Support Contractor*



*PRiME 2024*

*Oct. 8, 2024*

# Disclaimer



This project was funded by the United States Department of Energy, National Energy Technology Laboratory, in part, through a site support contract. Neither the United States Government nor any agency thereof, nor any of their employees, nor the support contractor, nor any of their employees, makes any warranty, express or implied, or assumes any legal liability or responsibility for the accuracy, completeness, or usefulness of any information, apparatus, product, or process disclosed, or represents that its use would not infringe privately owned rights. Reference herein to any specific commercial product, process, or service by trade name, trademark, manufacturer, or otherwise does not necessarily constitute or imply its endorsement, recommendation, or favoring by the United States Government or any agency thereof. The views and opinions of authors expressed herein do not necessarily state or reflect those of the United States Government or any agency thereof.

**Fei Xue<sup>1,2</sup>; Yinkai Lei<sup>1,2</sup>; Tian-Le Cheng<sup>1,2</sup>; Tao Yang<sup>3,4</sup>; William K. Epting<sup>1</sup>; Harry Abernathy<sup>3</sup>;  
You-Hai Wen<sup>1</sup>**

**<sup>1</sup>National Energy Technology Laboratory, 1450 Queen Avenue SW, Albany, OR 97321, USA**

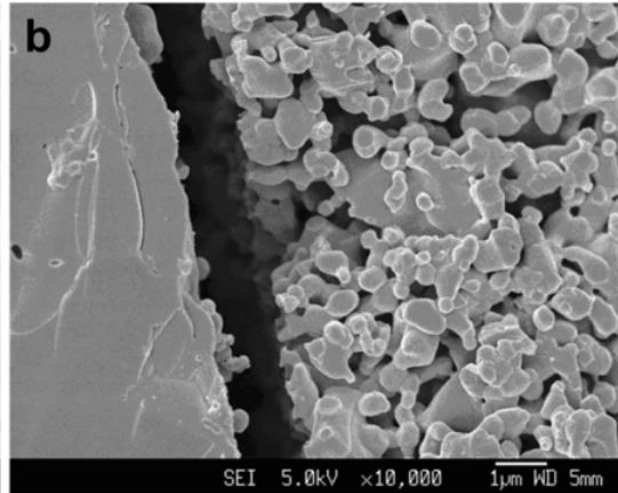
**<sup>2</sup>NETL Support Contractor, 1450 Queen Avenue SW, Albany, OR 97321, USA**

**<sup>3</sup>National Energy Technology Laboratory, 3610 Collins Ferry Road, Morgantown, WV 26505,  
USA**

**<sup>4</sup>NETL Support Contractor, 3610 Collins Ferry Road, Morgantown, WV 26505, USA**

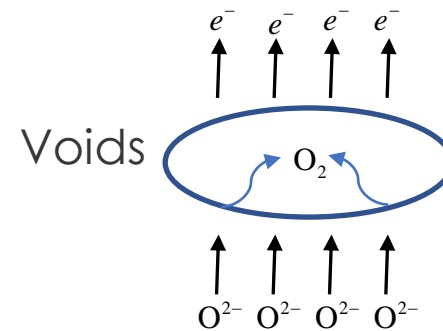
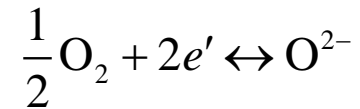
# Delamination of LSM-Based Oxygen Electrode

## LSM delamination under electrolysis

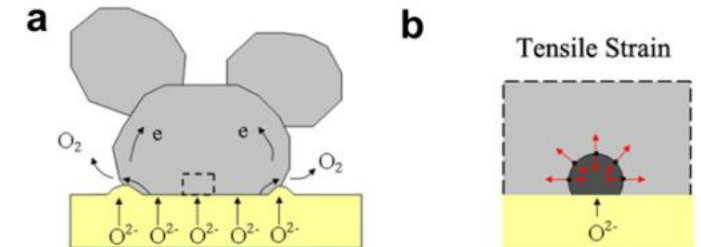


## Two popular mechanisms

Inner oxygen pressure



Lanthanum strontium manganate (LSM) lattice shrinkage due to oxygen vacancy accumulation



The first mechanism becomes dominant in recent years, which explains some experimental results.

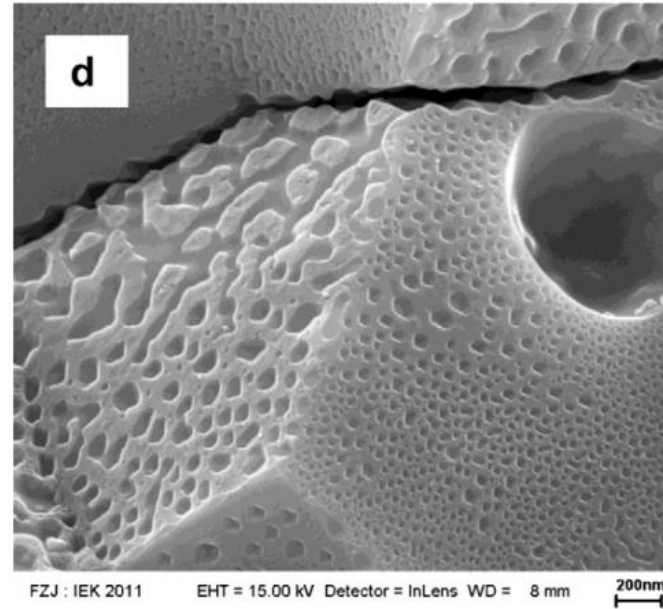
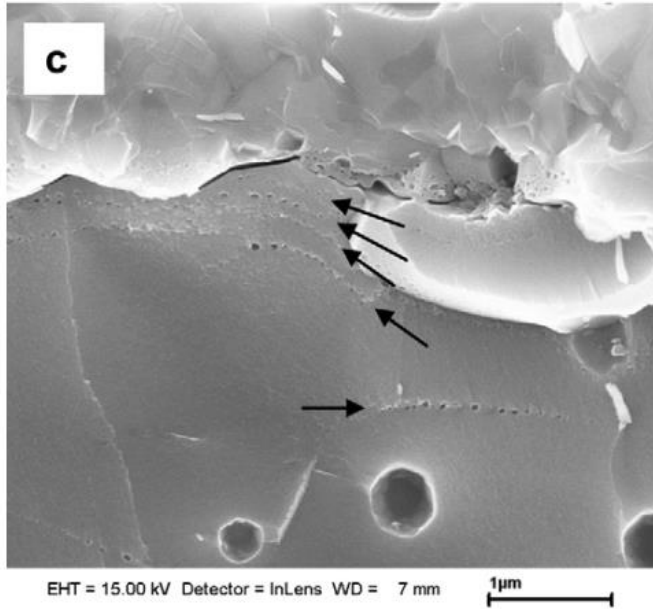
The stress from the second mechanism is not large enough to cause delamination even if the oxygen vacancy concentration is extreme high.

Int. J. Hydrogen Energy 36 (2011) 10541.

# Mechanical Degradation in LSCF-Based Cells

Pore formation in YSZ

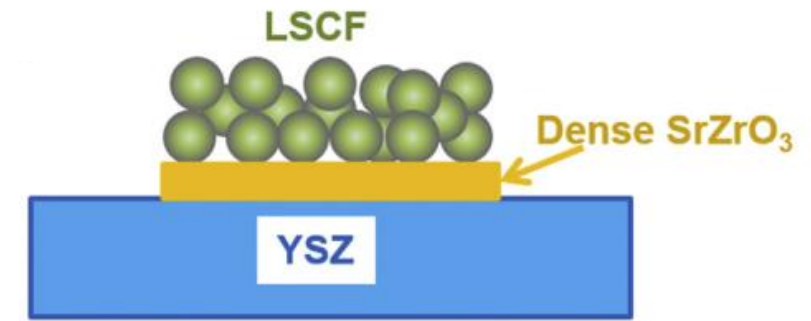
Intergranular fracture in YSZ



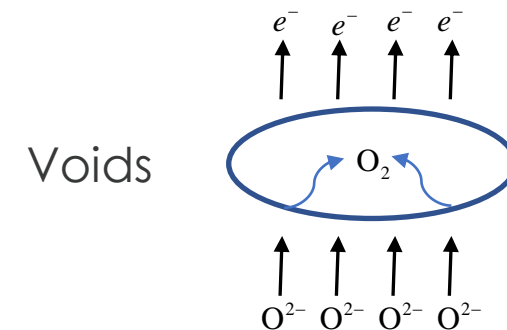
*Journal of Power Sources* 223 (2013) 129-135.

LSCF: lanthanum strontium cobalt ferrite.  
YSZ: yttria stabilized zirconia.

Two popular mechanisms  
Formation of secondary phases



Inner oxygen pressure



Pore formation, intergranular fracture in electrolyte, and electrode delamination are observed.

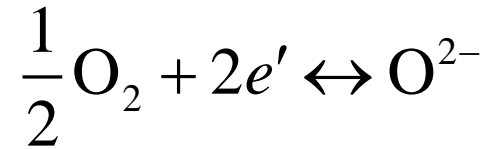
*International Journal of Hydrogen Energy* 43, no. 11 (2018): 5437-5450.

# Extend Virkar's Model by Incorporating the Microstructures

The key idea of Virkar's model: the electronic current within the electrolyte should be considered.

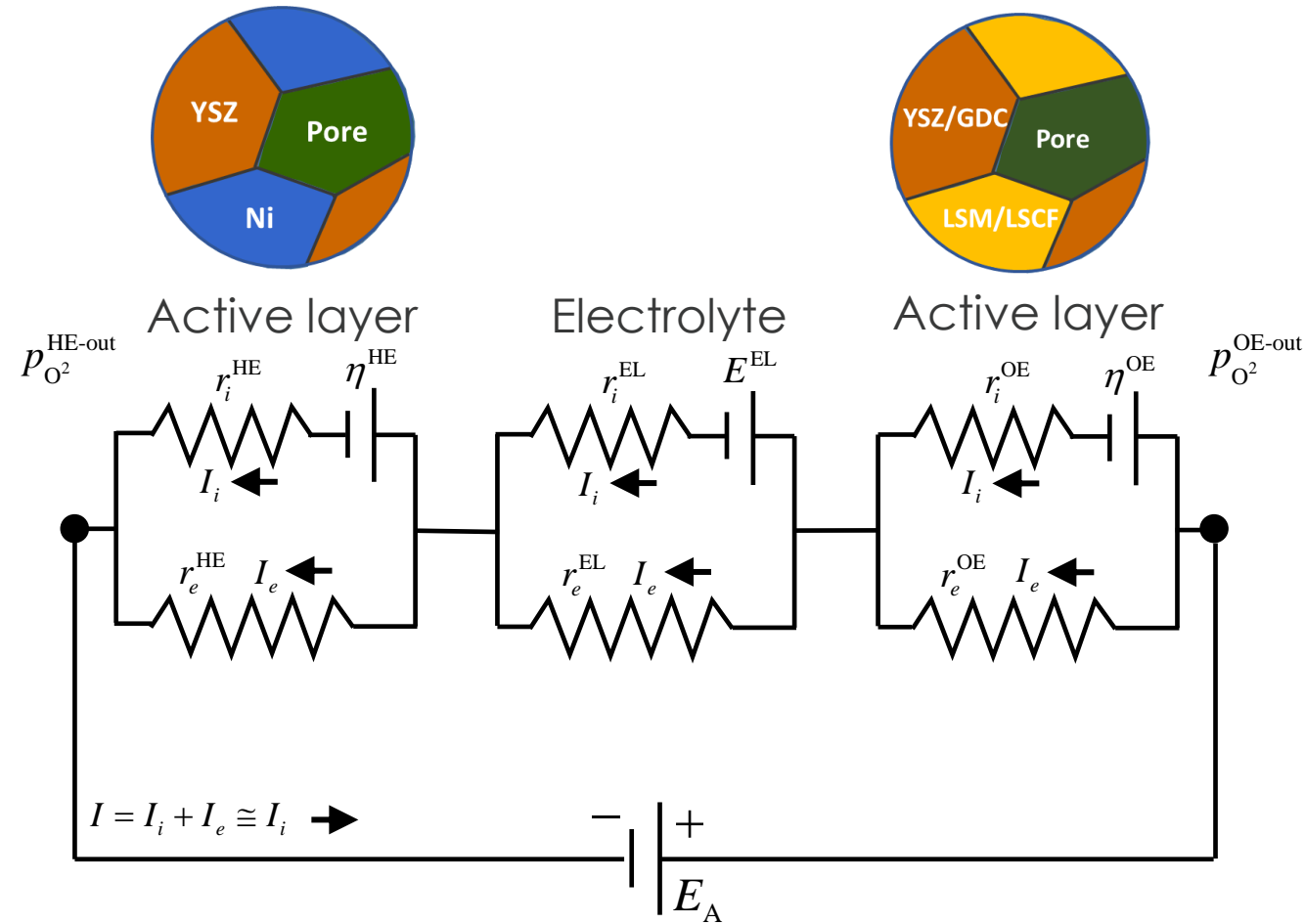
A. V. Virkar, *Int. J. Hydrogen Energy*, 35, 9527 (2010)

The inner oxygen pressure can be calculated based on the chemical equilibrium of:



Advantages of Yinkai's model:

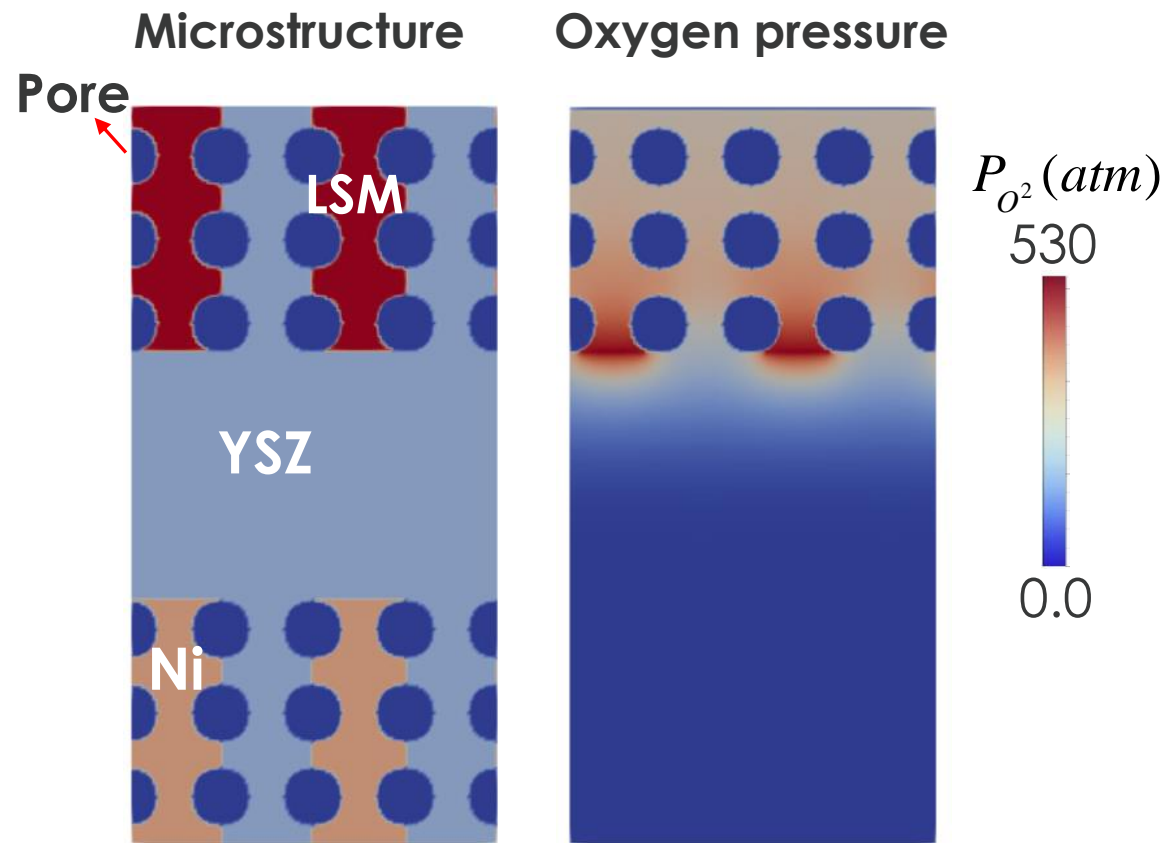
- The microstructures are considered
- Chemical reactions at triple-phase-boundaries (TPBs) and 2-phase-boundaries are described by Butler-Volmer Equations



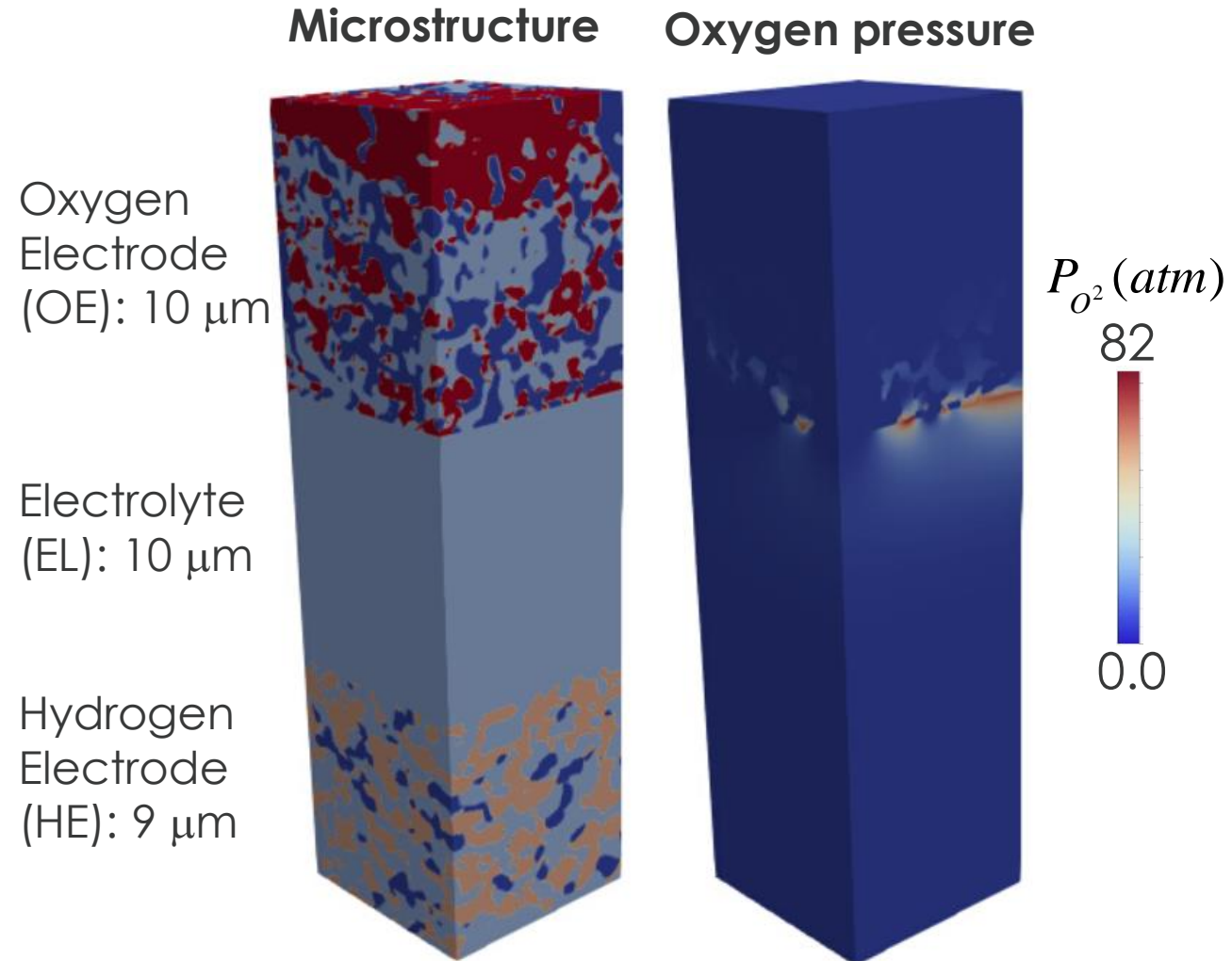
GDC: gadolinia-doped ceria.

Y. Lei et al. *ECS Transactions*. 2023;111:965.

# Two Types of Microstructures: 2D Preset and 3D Reconstructed

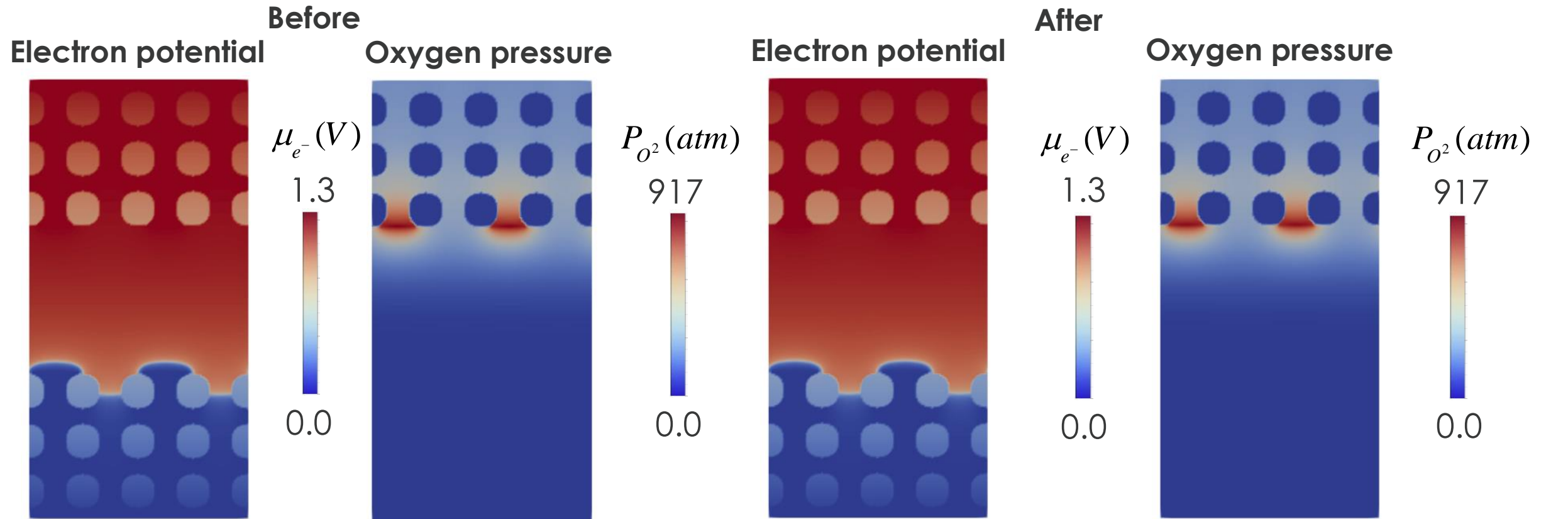


The maximum of oxygen pressure is achieved at the OE-EL interface.



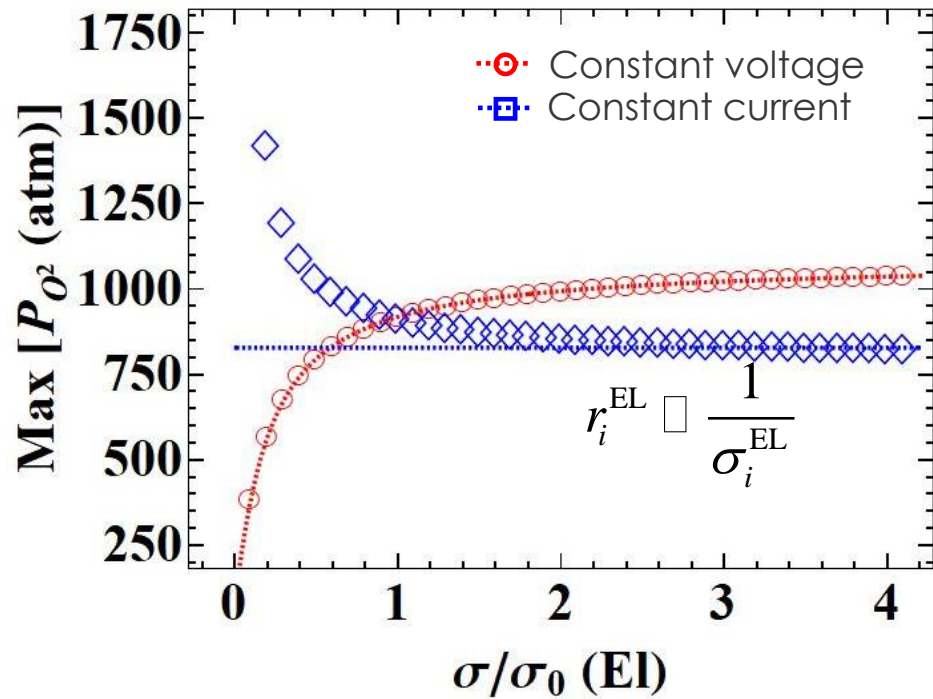
# Influence of Tuning Electronic Transport Properties of YSZ

Multiply the  $e^-$  conductivity of YSZ by 2,000 times, following Lei Zhang et. al J ECS, 166 (2019) F1275-F1283.



$$p_{O_2}^{OE-EL} = p_{O_2}^{Ox} \exp\left[\frac{4F}{RT} \left\{ \frac{r_i^{OE}}{r_i^{OE} + r_e^{EL} + r_i^{HE}} (E_A - E_N) - \frac{r_e^{OE}}{r_e^{OE} + r_e^{EL} + r_e^{OE}} E_A \right\}\right] \xrightarrow{r_e^{OE} \sim 0} p_{O_2}^{OE-EL} = p_{O_2}^{Ox} \exp\left[\frac{4F}{RT} \left\{ \frac{r_i^{OE}}{r_i^{OE} + r_i^{EL} + r_i^{HE}} (E_A - E_N) \right\}\right]$$

# Influence of the O<sup>2-</sup> Conductivity of the YSZ Electrolyte Based on 2D Simulations



The dashed lines are obtained by fitting the analytical solution.

$$p_{O_2}^{OE-EL} = p_{O_2}^{Ox} \exp\left[\frac{4F}{RT} \left\{ \frac{r_i^{OE}}{r_i^{OE} + r_i^{EL} + r_i^{HE}} (E_A - E_N) \right\}\right]$$

Deviation at small O<sup>2-</sup> conductivity under galvanostatic operation is due to the change of  $r_i^{OE}$ .

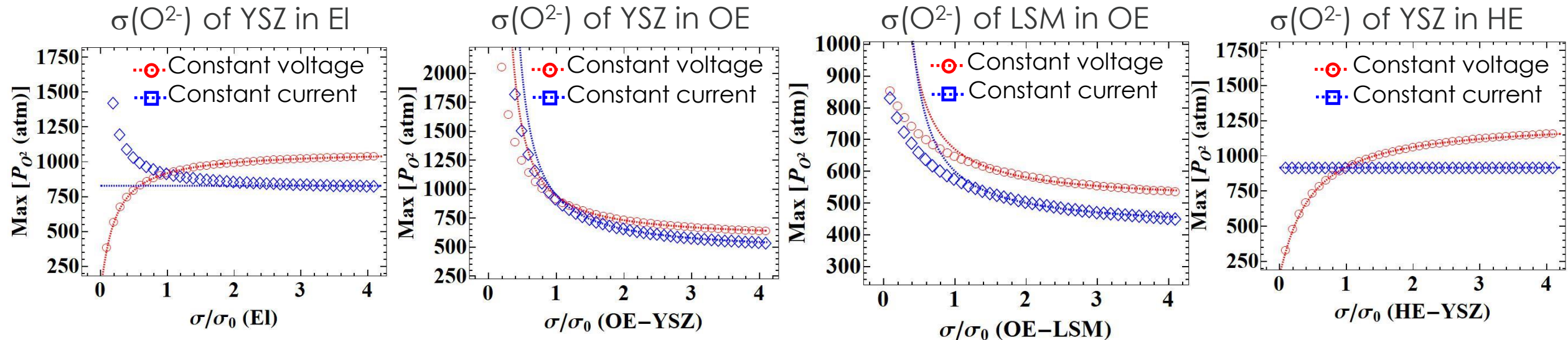
$r_i^{OE}$  is effective resistance including the reaction resistance.

$\sigma(O^{2-})$  of the electrolyte should be small under potentiostatic operation and large under galvanostatic operation.

The analytical solution can be employed to fit to the simulation results, but cannot predict the specific values before fitting, since  $p_{O_2}^{Ox}$ ,  $r_i^{OE}$ , and  $r_i^{HE}$  are unknown and fitting parameters.

# Influence of Tuning the O<sup>2-</sup>- Conductivity of YSZ and LSM

Tuning the O<sup>2-</sup>- conductivity of YSZ and LSM using 2D simulations (constant voltage vs. constant current).



$$p_{O_2}^{OE-EL} = p_{O_2}^{Ox} \exp\left[\frac{4F}{RT} \left\{ \frac{r_i^{OE}}{r_i^{OE} + r_i^{EL} + r_i^{HE}} (E_A - E_N) \right\}\right]$$

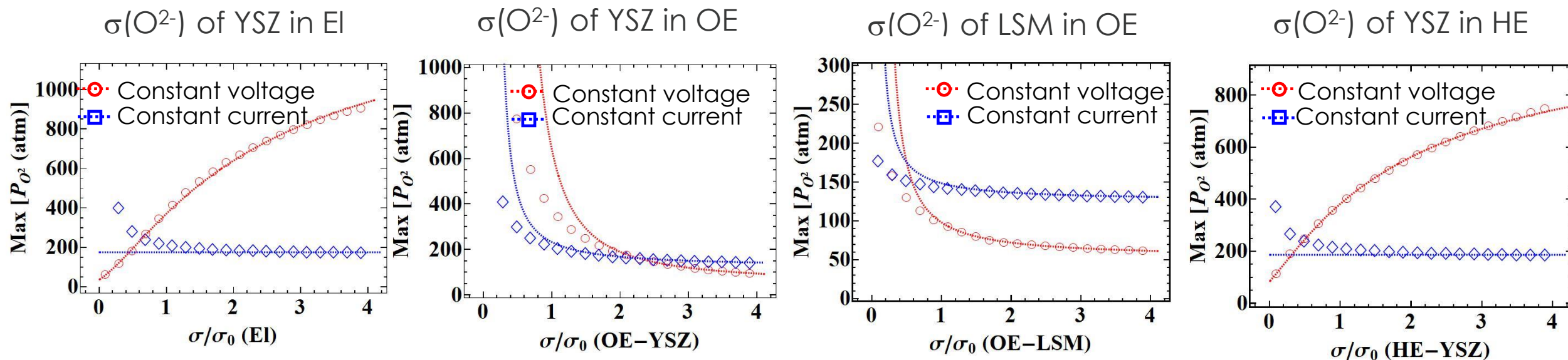
$$r_i \propto \frac{1}{\sigma_i}$$

V=1.3 V for constant voltage.

Under potentiostatic operation, σ(O<sup>2-</sup>) of YSZ in EI and HE: small; σ(O<sup>2-</sup>) of YSZ in OE and LSM: large.  
 Under galvanostatic operation, σ(O<sup>2-</sup>) of LSM and YSZ in EI and OE should be large.  
 The simulation results are qualitatively consistent with the analytical solution.

# Influence of Tuning the O<sup>2-</sup>- Conductivity of YSZ and LSM from 3D Simulations

Tuning the O<sup>2-</sup> conductivity of YSZ and LSM using 3D simulations (constant voltage vs. constant current).

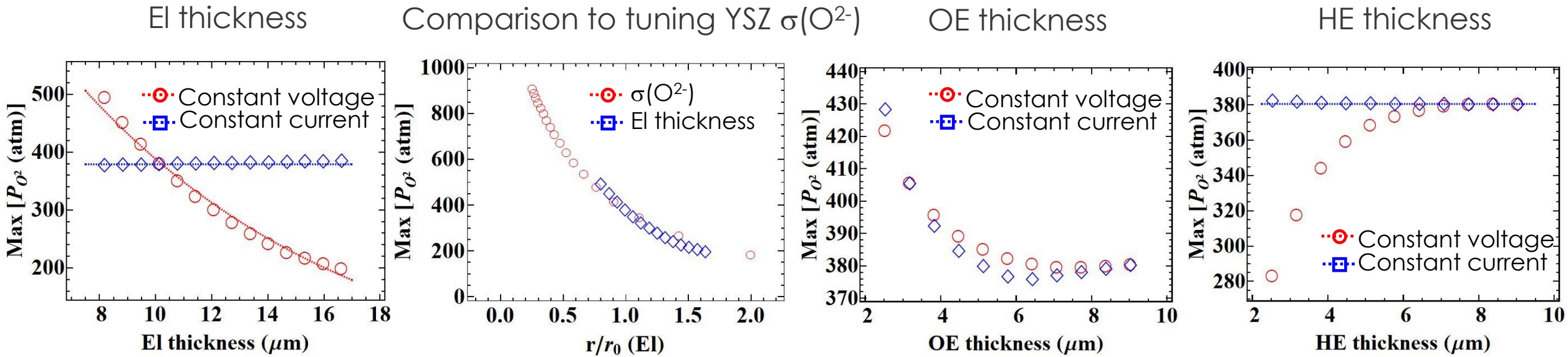


V=1.3 V for constant voltage.

Under potentiostatic operation,  $\sigma(\text{O}^{2-})$  of YSZ in EI and HE: small;  $\sigma(\text{O}^{2-})$  of YSZ in OE and LSM: large.  
 Under galvanostatic operation,  $\sigma(\text{O}^{2-})$  of LSM and YSZ in EI and OE should be large.  
 The results from 3D simulations are consistent with those from 2D simulations.

# Influence of Tuning the Electrode/Electrolyte Thickness

Tuning the electrode/electrolyte thickness using 3D reconstructed microstructures.

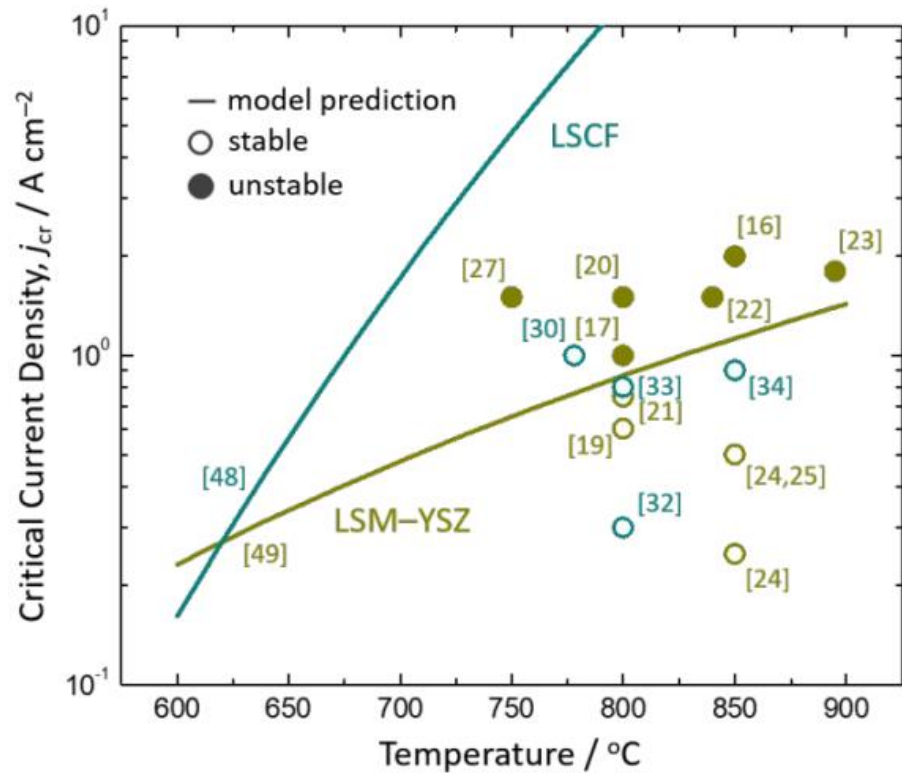


$V=1.3$  V for constant voltage.

Under constant voltage, thicker electrolyte, thicker OE, and thinner HE are favored.

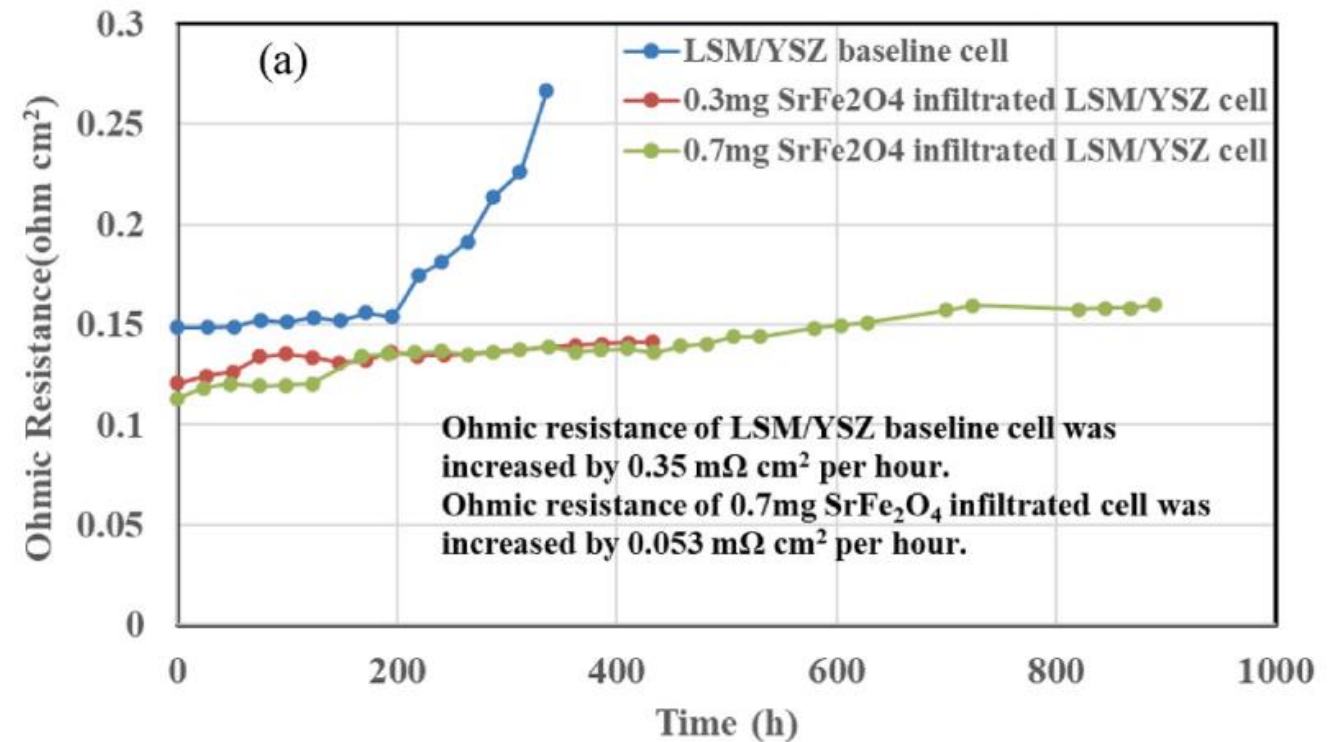
Under constant current, thinner electrolyte, an intermediate OE thickness, and thicker HE are favored.

## Mixed conductor LSCF mitigates delamination



Energy & Environmental Science. 2019;12:3053-62.

## Infiltration changes the effective conductivity of LSM



Y. Fan et al. Journal of Power Sources 580 (2023) 233389.

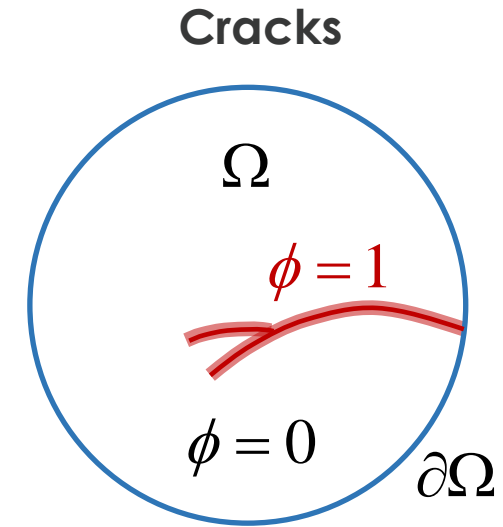
# Phase-Field Fracture Model and Coupled Performance-Crack Model

Total free energy for the phase-field fracture model:

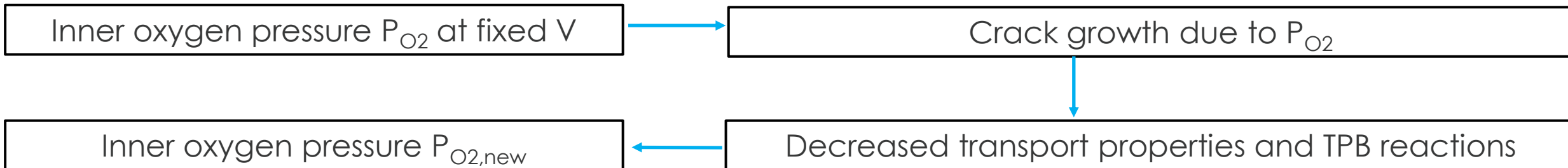
$$F = \int_{\Omega} [f_{\text{elas}}(\phi) + f_{\text{frac}}(\phi)] d\Omega$$

The elastic energy  $f_{\text{elas}}$  is the driving force of crack growth and may decrease after crack growth.

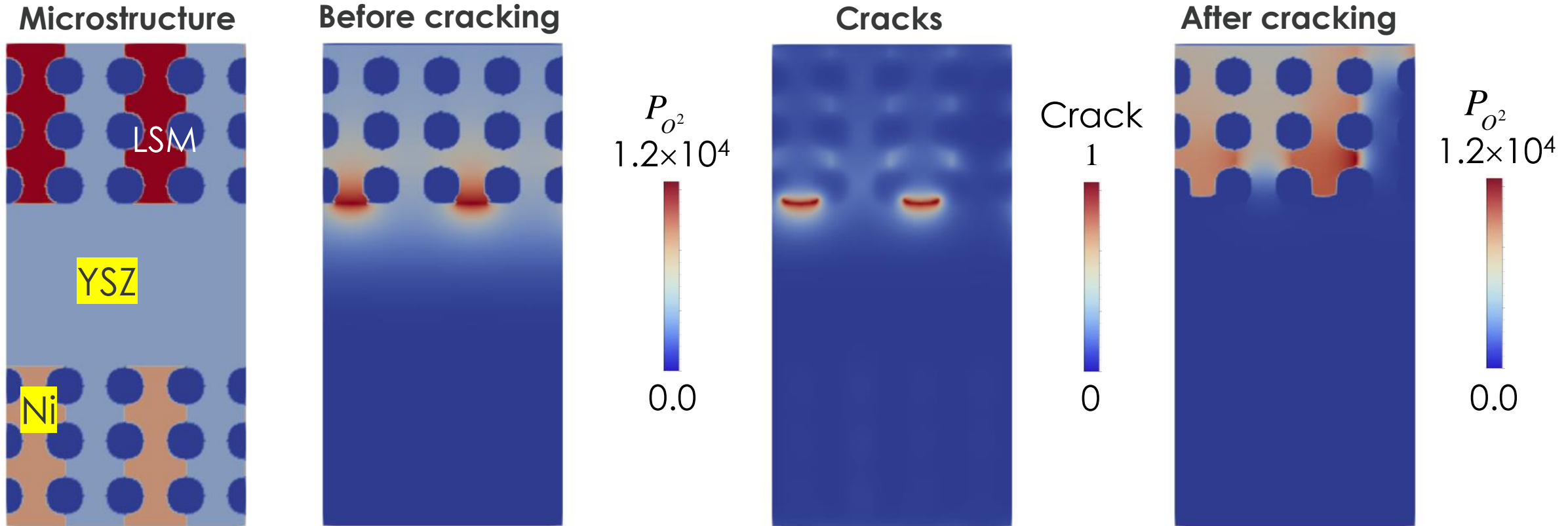
The fracture energy  $f_{\text{frac}}$  represents the fracture surface energy due to crack growth.



## Coupled performance-crack model at fixed voltage



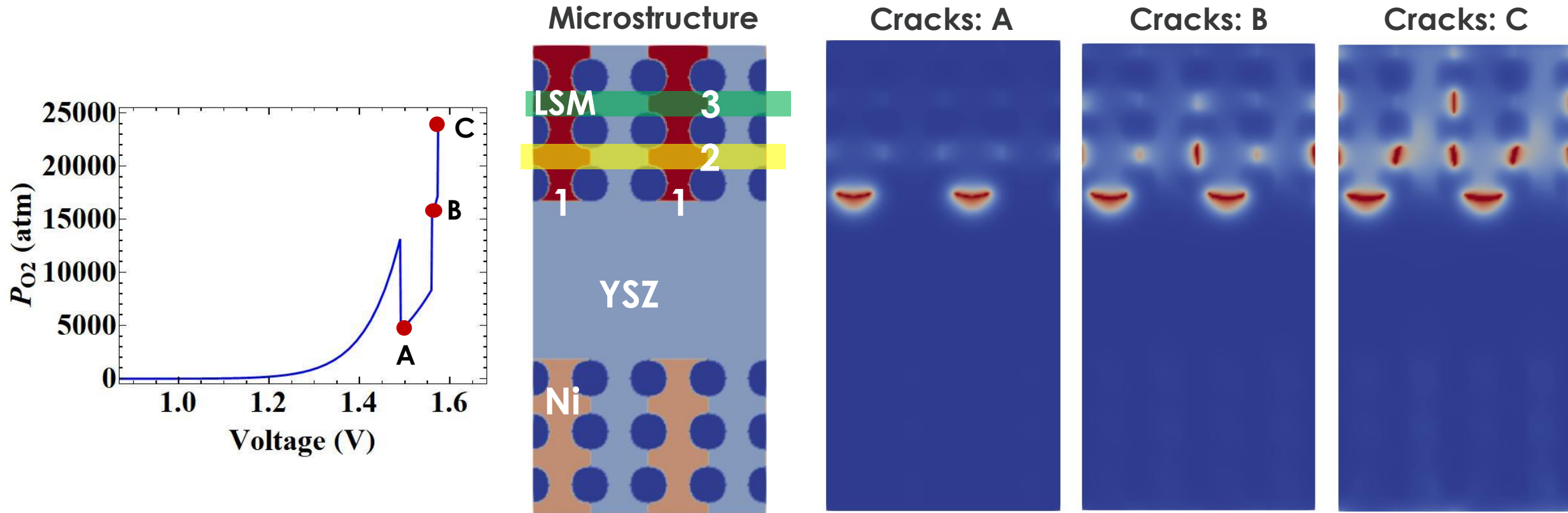
# Coupled Performance-Fracture Model at Fixed Voltage



The simulation is performed at  $V=1.47$  V.

After cracking, the maximum of oxygen pressure is achieved inside the OE, which suggests layer-by-layer cracking.

# Crack Growth in LSM-based Cells Under Changing Voltage



After crack growth at the OE-EL interface, the maximum of oxygen pressure is achieved at the LSM-YSZ interface inside the OE. Then layer-by-layer cracking is observed.

Conclusions from the parametric studies of inner oxygen pressure in LSM-based cells:

1. Different from the conclusions by Virkar et al. and Zhang et al., increasing the electronic conductivity of YSZ cannot decrease inner oxygen pressure from our simulation results.
2. Under potentiostatic operation, the following conditions are favored: (1) smaller ionic conductivity of YSZ in the electrolyte and HE; (2) larger ionic conductivities of LSM and YSZ in the OE; (3) thicker electrolyte; (4) thicker OE; and (5) thinner HE.
3. Under galvanostatic operation, the following conditions are favored: (1) larger ionic conductivity of YSZ in the electrolyte and OE; (2) larger ionic conductivity of LSM; (3) thinner electrolyte; and (4) an intermediate thickness of the OE.

Conclusions from the coupled performance-fracture model:

1. Crack growth is induced at the interfaces with high inner oxygen pressure.
2. After crack growth, the inner oxygen pressure is redistributed. Simulation results suggest layer-by-layer cracking in the LSM-based cells.

# Acknowledgments

---

This work was performed in support of the U.S. Department of Energy's (DOE) Office of Fossil Energy Crosscutting Technology Research Program. This work was performed in support of the U.S. DOE's Hydrogen and Fuel Cell Technologies Office (HFTO)'s H2NEW Program. The research was executed through the NETL Research & Innovation Center's Solid Oxide Fuel Cell Research Program.

The authors are grateful to Drs. Xingbo Liu and David S. Mebane for valuable discussions.

Thanks for your attention!

Questions?

# NETL RESOURCES

---

VISIT US AT: [www.NETL.DOE.gov](http://www.NETL.DOE.gov)

 @NETL\_DOE

 @NETL\_DOE

 @NationalEnergyTechnologyLaboratory

CONTACT:

Fei Xue

Fei.Xue@netl.doe.gov



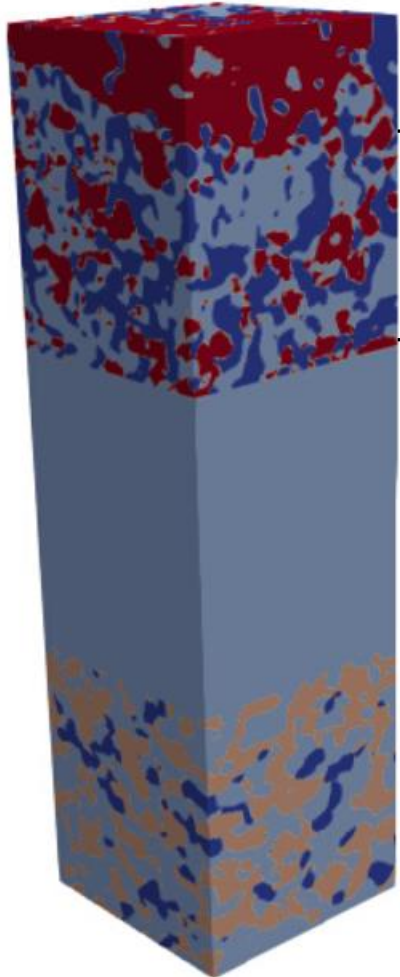
# Backup Slides

---



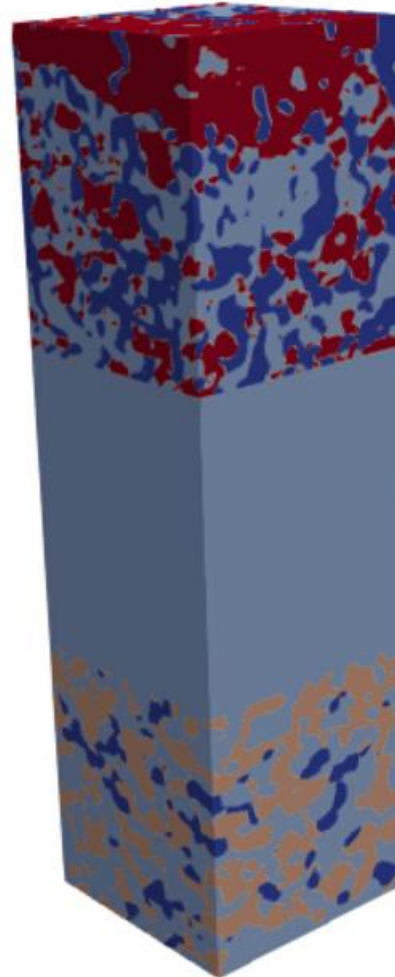
# Tuning the Thickness of the Electrode/Electrolyte

Tuning OE thickness



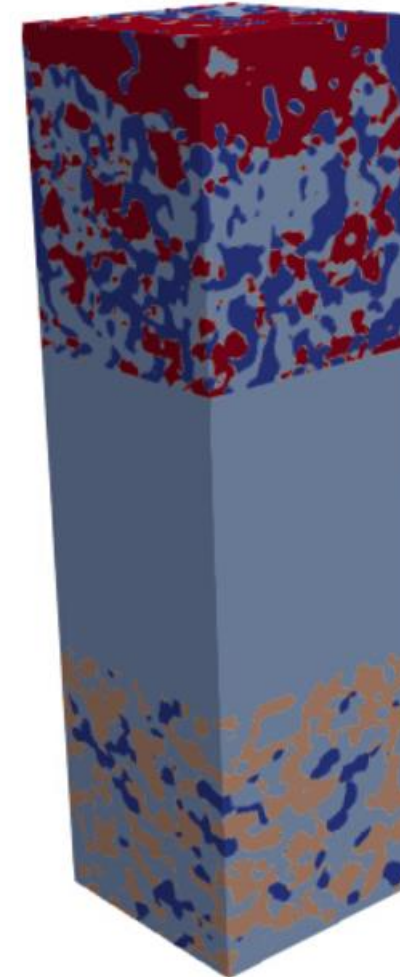
Take a  
section

Tuning electrolyte thickness



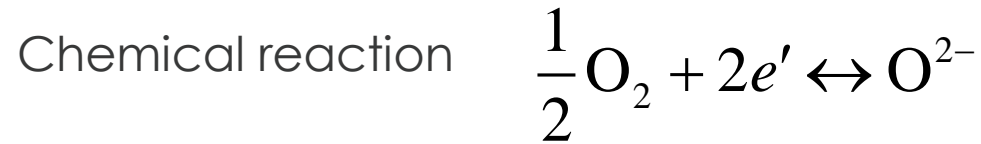
Tuning  
thickness

Tuning HE thickness



Take a  
section

# Extend Virkar's Model by Incorporating the Microstructures



Conduction equation for oxygen ions  $0 = \nabla \cdot [-\sigma_{O^{2-}}(\xi_i) \nabla \phi_{O^{2-}}] - i_F$

Conduction equation for electrons  $0 = \nabla \cdot [-\sigma_{e^-}(\xi_i) \nabla \phi_{e^-}] + 2i_F$

The source term at TPB: Butler-Volmer Equations

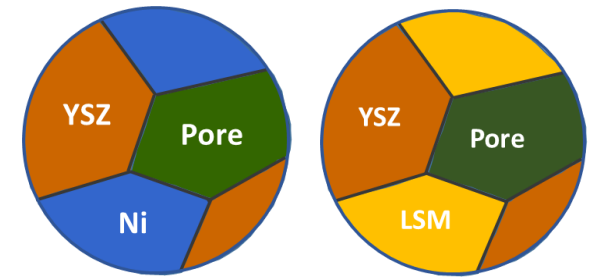
$$i_{F,c} = i_{0,c} \left( \frac{P_{O_2}^{\text{Pore}}}{P_{\text{ref}}} \right)^{0.25} \left\{ \exp\left[-\frac{\alpha n F \eta_c}{RT}\right] - \exp\left[\frac{(1-\alpha)n F \eta_c}{RT}\right] \right\}$$

Local overpotential at TPBs  $\eta_c = -\phi_{O^{2-}, \text{YSZ}} + \phi_{e^-, \text{LSM}} - \frac{RT}{4F} \ln \frac{P_{O_2}^{\text{Pores}}}{P_{O_2}^0}$

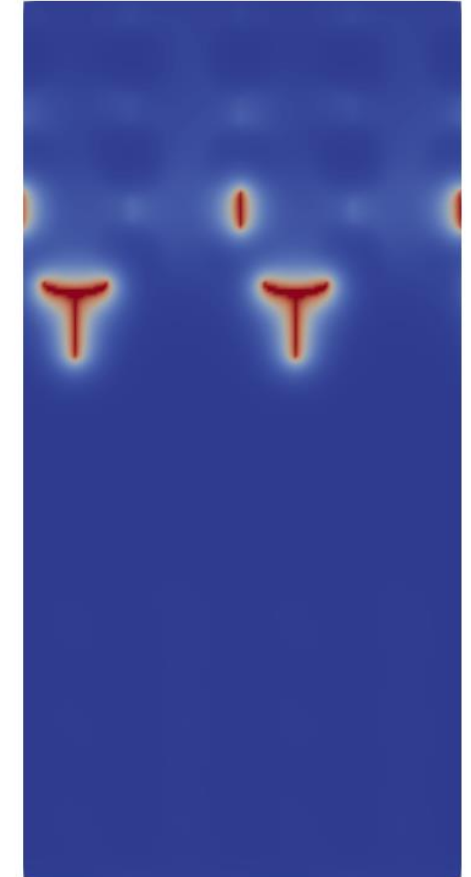
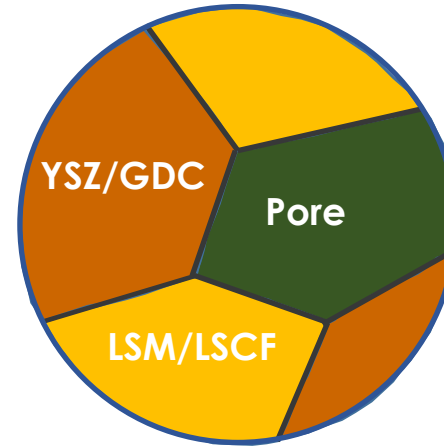
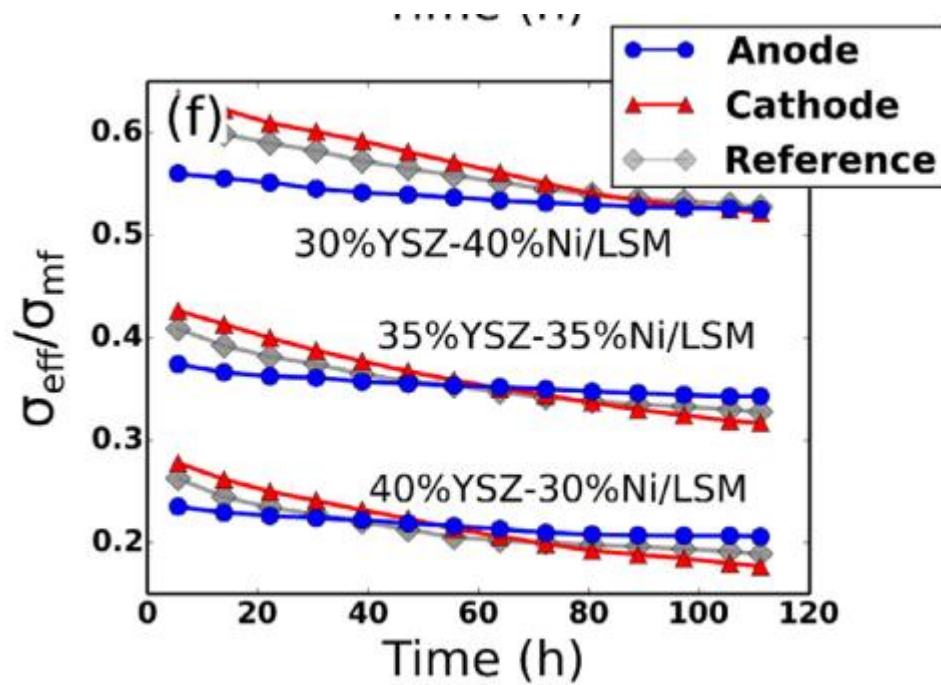
Gas diffusion within the pores is neglected

Inner oxygen pressure  $P_{O_2} = P_{O_2}^0 \exp\left[\frac{4F}{RT} (\phi_{e^-} - \phi_{O^{2-}})\right]$

HE and OE microstructures



# Effective Conductivity of the Electrodes

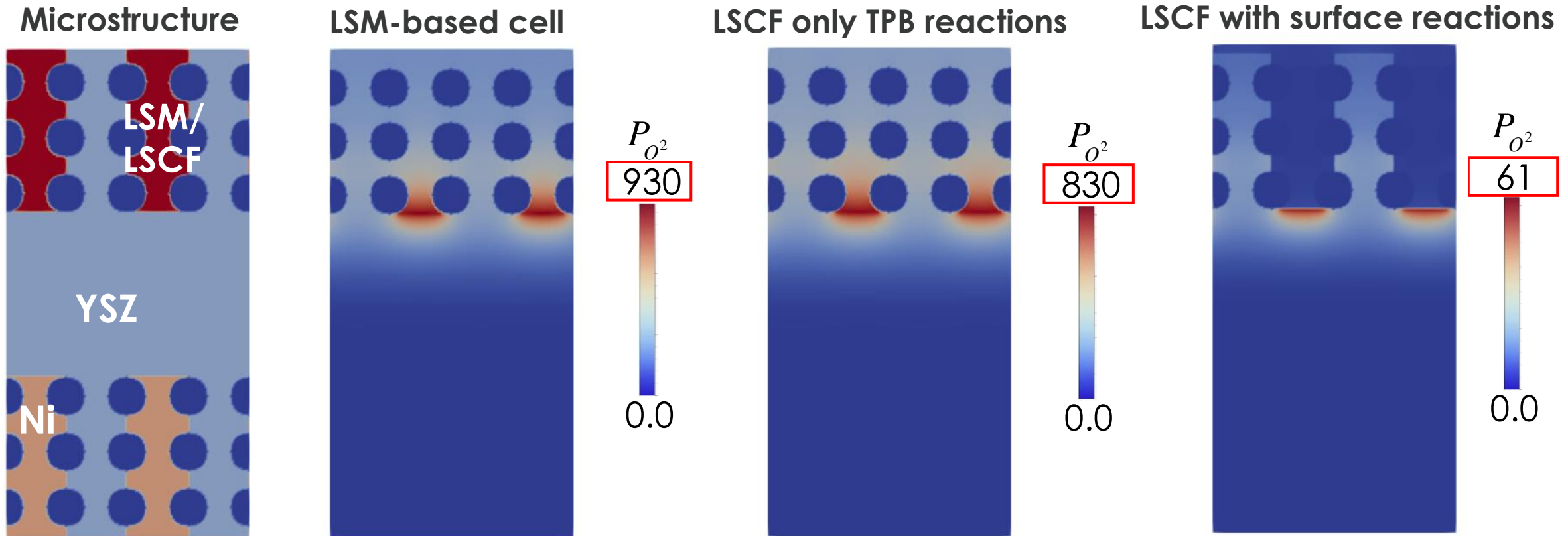


From Y. Lei et al./Journal of Power Sources 345 (2017) 275-289.

# Oxygen Pressure in LSM- and LSCF-Based cells

$$V_{\text{cell}} = 1.3 \text{ V}, \quad i_0^{\text{NiYSZTPB}} = 2.345 \times 10^{-3} \text{ A} \cdot \text{m}^{-1} \quad i_0^{\text{LSMYSZTPB}} = 2.247 \times 10^{-4} \text{ A} \cdot \text{m}^{-1} \quad i_0^{\text{LSCFYSTPB}} = 2.247 \times 10^{-4} \text{ A} \cdot \text{m}^{-1}$$

$$i_0^{\text{LSCFSurface}} = 2.0 \times 10^{-4} \text{ A} \cdot \text{m}^{-1} \quad i_0^{\text{LSCFYSZInterface}} = 3.0 \times 10^{-4} \text{ A} \cdot \text{m}^{-1}$$



Oxygen pressure is lower in LSCF-based cells than that in LSM-based cells.